Impulse Response Measurement and Mode Shapes of a Violin

Noah Saxenian

December 11, 2025

Tufts University

Mechanical Engineering

ME126 Final Paper

Abstract

The purpose of this lab was to perform modal analysis of a violin top plate, compare mode shapes with existing literature, and evaluate the performance of the analysis tools. Using a roving hammer impact test and laser vibrometer measurements, frequency response functions were collected at 75 locations and processed with a custom circle-fitting algorithm to extract modal parameters. These parameters were used to reconstruct and visualize mode shapes, from which the CBR, A1, and B1+ signature modes were identified. Understanding the modal behavior of violin bodies helps relate vibration patterns to the acoustic qualities of the instrument.

Introduction

As a continuation of the research conducted in Professor Rogers' lab, this project involved conducting a roving hammer impact test on the top plate of a violin body and using the modal analysis tools previously developed to reconstruct its mode shapes. This is an extension of my previous work performing this type of test and analysis on a simple metal plate.

A violin's characteristic tone is heavily influenced by how its top and bottom plates vibrate. Understanding these plate dynamics can give insight into why violins can sound so different relative to each other. Violin plates are especially interesting for testing because their geometry and material properties create a complex and sensitive acoustic system, where slight variations in thickness or shape can drastically alter the sound.

The primary goal of this measurement is to extract modal parameters of the violin body from its frequency response at multiple different locations and process these parameters to create visualizations of different mode shapes. Additionally, it would serve to validate the experimental setup and analysis tools, primarily through the comparison of mode shape visualizations with existing literature. It is expected that the major signature modes (A0, CBR/C2, B1–, and B1+) will be identifiable within typical frequency ranges.

Methods

A roving hammer test was performed using a model 086E80 impact hammer from PCB Piezotronics with a rubber tip and a Polytec IVS-500 laser vibrometer. The violin body was mounted vertically in an adjustable tripod setup with the base resting on a rubber mat and the neck held suspended by rubber bands to simulate a free boundary condition. The laser vibrometer was positioned to focus on a single response point. As shown in Figure 1, the hammer was then used to impact each target location.

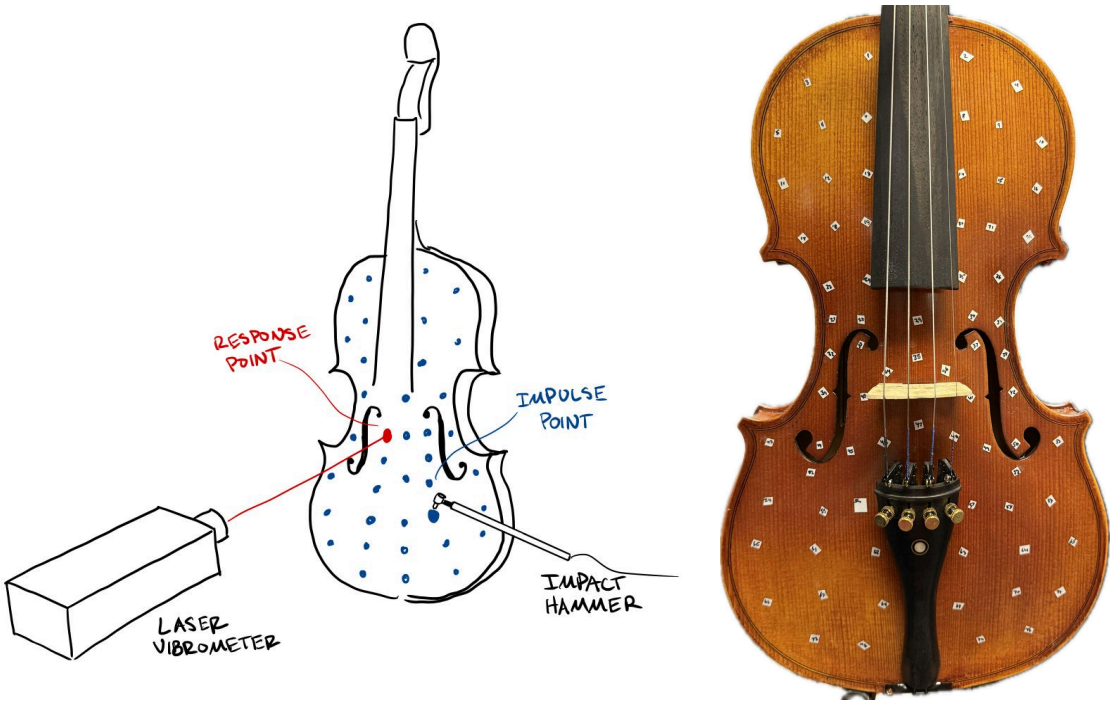

Figure 1: Diagram of Modal Impact Testing Setup (left) and Measurement Locations (right)

A grid of 75 locations was marked out on the top plate of the violin. A piece of retro-reflective tape was applied at location 56 to provide a good reflection for the laser at the response point. Each of the locations was tapped five times by hand using the impact hammer. Five taps were chosen to balance averaging quality and time. Signal processing was done with the Oberlin Acoustics LabVIEW software, acquiring 1 second samples of data at a rate of 48000 samples/second [1]. This software also computes the frequency response function and coherence from an average of the five taps. The coherence function was plotted during testing to validate the consistency of these hits and avoid outliers, as mentioned in [2]. Based on both the coherence plots and the fourier transform of the hammer response, bad hits were identified by eye and retaken immediately. As discussed in [3], this roving hammer test generates a single row of an FRF matrix that can be used for modal analysis.

The resulting data was then processed with a python package that I previously wrote [4]. It fits curves to each frequency response function and extracts the modal parameters. The theory, as described in [5], uses the assumption that each resonant peak can be modelled as a single degree of freedom for a spring-mass system with structural damping.

$$Y(\omega) = i\omega \frac{A}{\omega_r^2 - \omega^2 + i\eta_r\omega_r^2} \tag{1}$$

Where A is the modal constant, ω_r is the natural frequency, and η_r is the damping coefficient. By fitting circles to the real vs. imaginary plots of the complex data, we can extract these modal parameters for each peak and reconstruct the frequency response function as a sum of all these SDOF equations. This is done for each pair of impulse and response points.

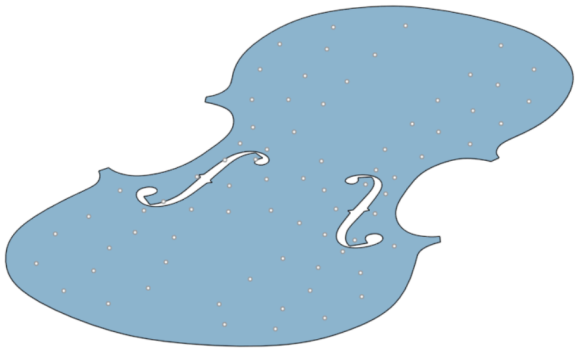

Figure 2: CAD model of the violin plate mesh and measurement locations.

To visualize mode shapes, an STL mesh of the violin top was created in CAD. A sketch of each of the measurement locations was made by tracing a photo of the experimental setup, then exported and used to extract the coordinates of these locations. The magnitude and phase of each mode shape at every measurement location is extracted from the modal constants, then interpolated over the rest of the mesh using a spline fit.

Results

The initial data collection was successful, resulting in 75 separate frequency response functions as well as an average of all points together (Figure 3).

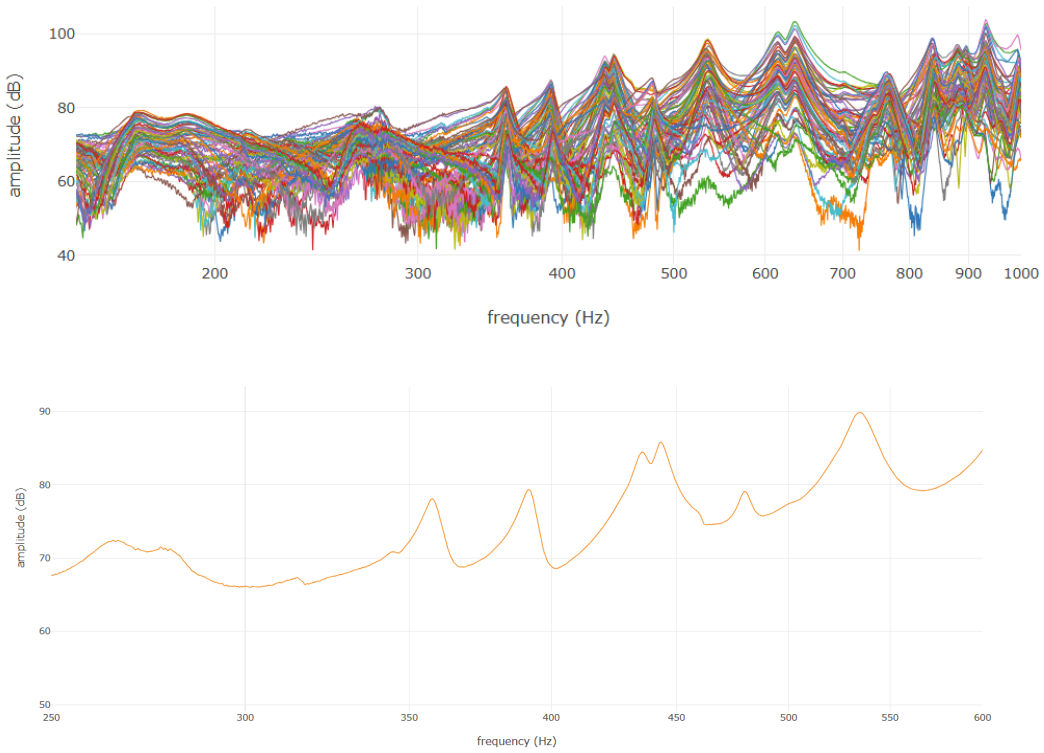

Figure 3: Individual Frequency Response Functions (Top), Average FRF (Bottom)

The resulting data was noisier than desired, especially at frequencies under 300 Hz. It was difficult to properly fit the curve for the first signature mode (A0), which should be around 270-290 Hz. Thus, the program was used to fit the FRFs from 300-600 Hz. Figure 4 shows the quality of fitted frequency response functions at two typical locations.

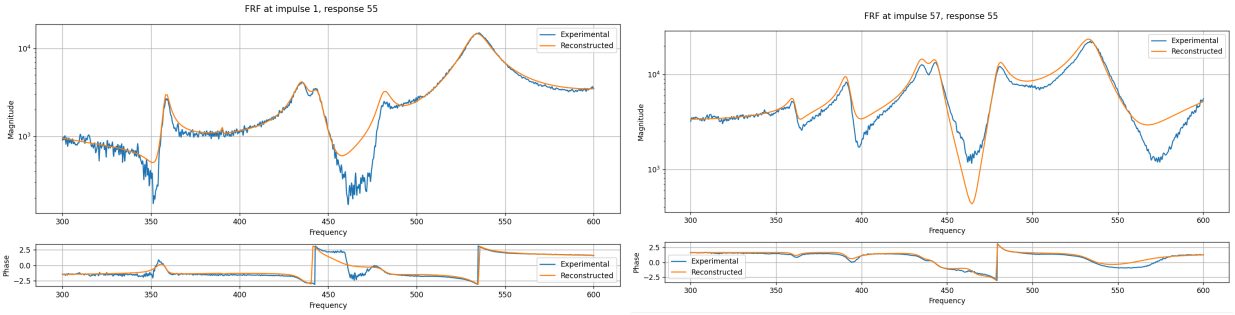

Figure 4: Example Fitted Frequency Response Functions

From the curve fits on all the points, six resonant frequencies were identified at 358 Hz, 392 Hz, 435Hz, 444 Hz, 480 Hz, and 535 Hz. Figure 5 shows the generated plots of mode shapes at each of these resonances.

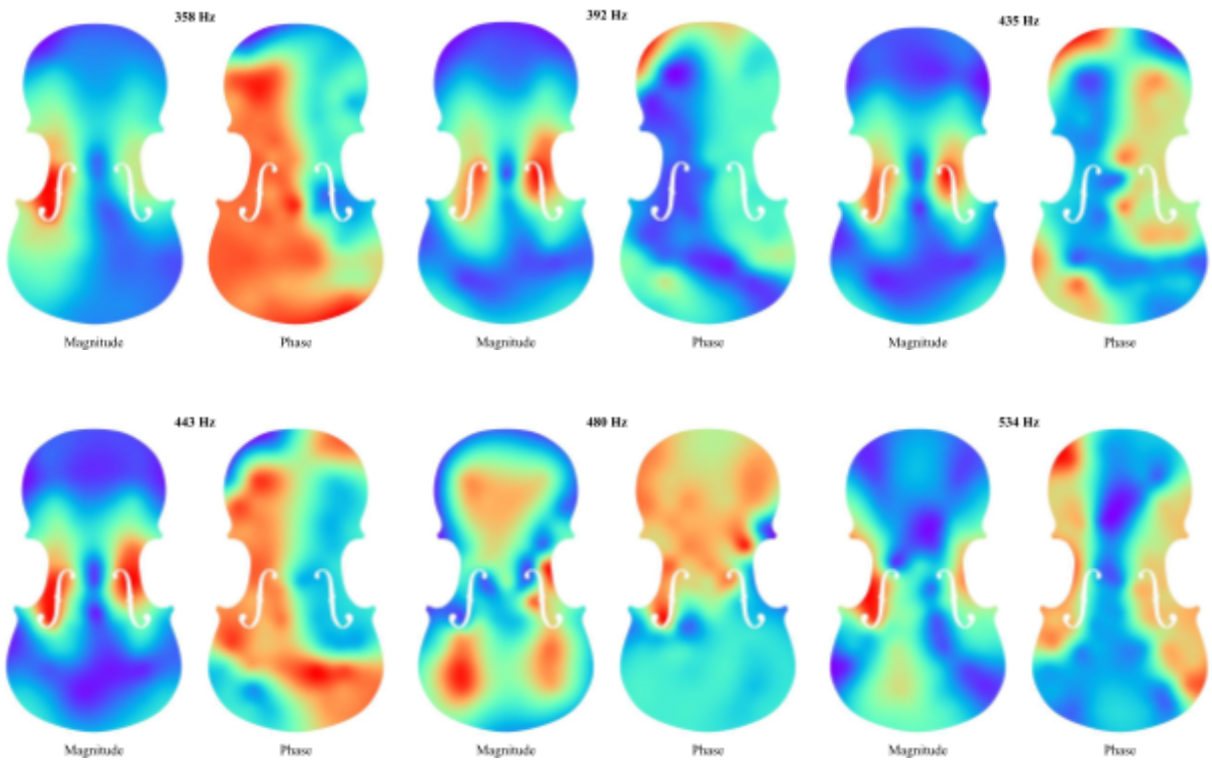

Figure 5: Mode Shape Plots of Magnitude and Phase at Each Identified Resonance

Discussion

The results show data with some clear trends and distinct mode shapes, indicating a successful test. Of the six identified modes (358, 392, 435, 444, 480, 535 Hz), it is expected that four in this range should align with the signature modes common to all violins reported by Schelske, Stoppani, and others [6, 7].

The peak at 392 Hz is likely the CBR mode (also called C2), which is normally between 380 and 420 Hz on most violins [7]. The high magnitude areas around the f-holes oscillating in opposite phase (Figure 5) are consistent with the literature, including the operating deflection shape of the C2 mode identified by Runnemalm et al. [9]. At 480 Hz, the A1 mode can be seen, distinct from flipped top and bottom phases. Additionally, the B1+ mode should be between 510 and 580 Hz, so it is identified as the peak found at 535 Hz [7]. However, it is difficult to distinctly identify the B1- (also called T1) mode.

The peaks at 435 and 444 Hz show similar magnitude patterns and flipped phase patterns (Figure 5). The patterns do not exactly match those seen in the literature. It is possible that these may represent the B-mode split into two peaks, however it is clearly not a computational artifact as the dual peaks show clearly

in the raw data across all locations. Additionally, the first identified mode at 358 Hz does not appear to have a great match in the first 25 eigenmodes charted by Schelske [6].

It is clear that the quality of data collected is sub-optimal. Noisy signals can be seen in most of the collected FRF's, and Figure 6 shows the coherence functions for several locations.

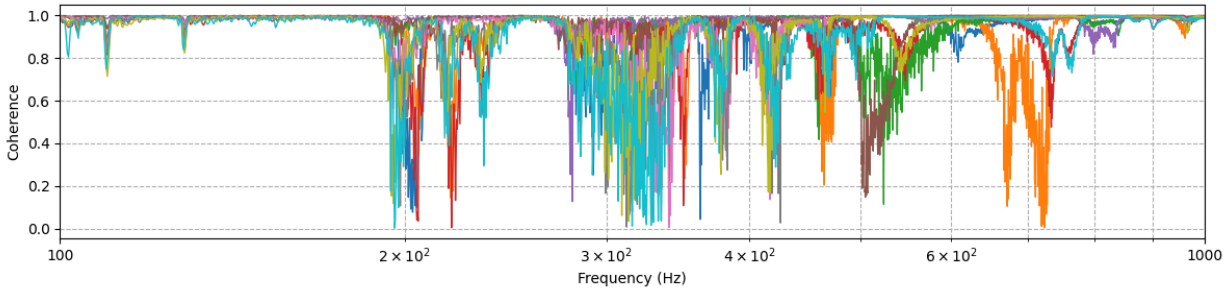

Figure 6: Coherence Functions Plotted for Select Locations

The coherence plot gives an indication of consistency of hits at the same measurement location, with values close to one indicating a high consistency in frequency response. Poor coherence could be due to a range of factors, discussed in further detail below.

Additionally, the amount of noise present below 300Hz (visible in Figure 3) made it difficult to get an adequate curve fit for the low frequencies. One of the most distinct signature modes is the A0 First Air Mode, which should be between 270-290 Hz [7]. Given the amount of noise in the low frequency range, it was determined that any analysis of the A0 mode in this violin would not be reliable.

Overall, modal parameter extraction was successful. Looking at the six resonant peaks identified, A custom quality factor metric to evaluate the success of the circle-fit method was defined as

$$Q_{\text{fit}} = 1 - 10\,\frac{\text{MSD}}{r^2} \tag{2}$$

where MSD is the mean squared deviation of the data and the fitted circle, and r is the circle radius to normalize for scale. Averaging this quality factor over all locations gives a sense for the quality of fit to each mode.

Resonant Frequency (Hz)	358	392	435	444	480	535
Average Quality Factor	0.97	0.94	0.96	0.98	0.97	0.94

Table 1: Average Quality Factor for each Fitted Resonant Peak

Overall, the averages shown in Table 1 show successful fitting, despite some variation and noisy data. It is worth noting, however, that one or two oddball failures would not throw the average far off, but would severely impact the mode shape interpolation and plots. Manual inspection of each fitted FRF verified the success, and peaks which were unable to be fit properly are treated as having no contribution to the FRF or mode shape.

There are many possible reasons for these discrepancies between the measured mode shapes and those found in previous studies. For one, the mass and stiffness of the violin plate used in this experiment is likely significantly different from those commonly measured. Often, really good violins are used in testing, as they represent a standard for other violins to compare to. While low quality violins should still exhibit the signature modes, they may present differently and be difficult to compare, and as Bissinger notes in a study on the comparison between structural acoustics of “good” and “bad” violins, the measurements do not always give the full picture of how humans rate the quality of sound [10].

Other sources of error in this experiment include the mounting conditions, noise, human inconsistencies, mesh resolution, and interpolation limitations. The violin was secured at the neck with rubber bands and with the base resting on a rubber pad, to simulate a nearly free boundary condition, but slight movement between hits could lead to inconsistencies in laser measurements. Some of the low frequency noise found in the measurements could be from unplanned motion of the whole violin body on its mount. Human inconsistencies were a large factor as well, as the hammer hits were done by hand. Slight variations in the location or angle of each hit was unavoidable, especially in hard to reach locations such as under the strings or near the bridge.

The mode shape visualizations were created through an interpolation of measurements across many more mesh points representing the surface of the violin. Interpolation has some severe limitations, as it creates the appearance of more data than is actually available, and it can be misleading. This is especially relevant around the f-holes, as the interpolation is done based on coordinate locations as opposed to distance along the surface of the mesh. A relatively low resolution of measurement locations can lead to misleading results.

Follow-up experiments would be useful to strengthen these results. Performing repeat taps using an automatic hammer actuator or pendulum system would greatly reduce the influence of human inconsistencies, and increasing measurement resolution around f-holes would help limit the impact of misleading mesh interpolations.

As an evaluation of the testing setup, software, and analysis tools, this experiment served to show high potential for future use of these tools. In particular, the circle-fitting python package performed especially well at reconstructing FRFs, even despite unideal data. With more care taken to gather lower-noise data, this process would run even more smoothly. The ability to generate mode shape images and animations, and interpolate these across a mesh is an incredibly powerful tool, although care must be taken to avoid misinterpretation of spline-based interpolation. Future users of this toolset will hopefully find it useful to perform circle-fit modal analysis on their own custom data.

Conclusion

The roving hammer test was conducted on a violin top plate successfully identified and fitted six main resonant peaks (358, 392, 435, 444, 480, and 535Hz). Several signature modes matched the literature (CBR/C2, A1, B1+) demonstrating the method's ability to capture modal features. However, other signature modes were ambiguous, and the low-frequency (A0) region was too noisy for reliable parameter extraction.

The test and analysis pipeline is determined to be valid and promising despite measurement noise. While low frequency noise obscured the lower modes and hammer tap inconsistencies reduced the reliability of collected data, these limitations point to clear avenues for future improvement. Automated hammer actuation and an improved mounting setup could greatly improve the quality of data across the whole frequency range. The circle-fit method shows strong accuracy even with imperfect data, but struggles with especially noisy regions and overlapping modes. The mode shape visualizations are effective but limited by measurement density and interpolation errors. Future testing should implement a higher resolution measurement grid, especially around complex geometry such as the f-holes.

Understanding the modal behavior of violin plates provides insight into how structural vibrations shape the instrument's acoustic characteristics. Future studies could extend this pipeline to full violin bodies or other stringed instruments. While sound perception is known to be a factor of more than just structural vibrations, refining these measurement and analysis techniques is necessary to deepen the connection between modal parameters and the acoustical qualities of the instrument.

References

[1] “Measuring Violin Acoustics,” *Oberlin Acoustics App*, Chris Rogers and Joseph Curtin, Google Sites. [Online]. Available: https://sites.google.com/view/oberlinacoustics/home. [Accessed: Nov. 6, 2025].

[2] M. H. Richardson, “Measurement and Analysis of the Dynamics of Mechanical Structures,” in *Proc. Hewlett-Packard Conf. for Automotive and Related Industries*, Detroit, MI, Oct. 1978. [Online]. Available: http://papers.vibetech.com/Paper04.pdf. [Accessed: Nov. 5, 2025].

[3] B. J. Schwarz and M. H. Richardson, “Experimental Modal Analysis,” in *Proc. CSI Reliability Week*, Orlando, FL, Oct. 1999. [Online]. Available: http://papers.vibetech.com/Paper28.pdf. [Accessed: Nov. 5, 2025].

[4] N. Saxenian, “CircleFit,” GitHub repository, https://github.com/noahsaxenian/CircleFit. [Accessed: Nov. 6, 2025].

[5] D. J. Ewins, *Modal Testing: Theory, Practice and Application*, 2nd ed. Baldock, Hertfordshire, England: Research Studies Press Ltd., 2000.

[6] M. Schleske, “Empirical Tools in Contemporary Violin Making: Part I. Analysis of Design, Materials, Varnish, and Normal Modes,” *Catgut Acoustical Society Journal*, vol. 4, no. 2, pp. 50–65, 2002. [Online]. Available: https://www.schleske.de/fileadmin/user_upload/doc/CAS_Empirical_I.pdf. [Accessed: Nov. 5, 2025].

[7] G. Stoppani and S. Zygmuntowicz, “Shapes of the Signature Modes,” Strad3D, Mar. 9, 2009. [Online]. Available: https://strad3d.org/st_2.html

[8] G. A. Knott, Y. S. Shin, and M. Chargin, “A modal analysis of the violin,” *Finite Elements in Analysis and Design*, vol. 5, no. 3, pp. 269–279, 1989, doi: 10.1016/0168-874X(89)90049-8. [Online]. Available: https://www.sciencedirect.com/science/article/pii/0168874X89900498

[9] A. Runnemalm, N.-E. Molin, and E. Jansson, “On operating deflection shapes of the violin body including in-plane motions,” *Journal of the Acoustical Society of America*, vol. 108, no. 1, pp. 347–356, 2000.

[10] G. Bissinger, “Structural acoustics of good and bad violins,” *Journal of the Acoustical Society of America*, vol. 124, no. 3, pp. 1764–1773, 2008, doi: 10.1121/1.2956478. [Online]. Available: https://strad3d.org/files/bissinger/JASA%202008%20Struct%20Acoust%20good%20bad%20violins.pdf